Sequential Bond Energies of $Cu(CO)_x^+$ and $Ag(CO)_x^+$ ($x = 1-4$)

Franc Meyer, Yu-Min Chen, and P. B. Armentrout*

Contribution from the Department of Chemistry, University of Utah, Salt Lake City, Utah 84112

Received October 31, 1994[⊗]

Abstract: The sequential bond energies of $Cu(CO)_x^+$ and $Ag(CO)_x^+$ ($x = 1-4$) are determined by collision-induced dissociation in a guided ion beam tandem mass spectrometer. Values (in eV) for the 0 K $(CO)_{x-1}Cu^+-CO$ bond energies are found to be 1.54 ± 0.07, 1.78 ± 0.03, 0.78 ± 0.04, and 0.55 ± 0.03 for $x = 1-4$, respectively, while those for $(CO)_{x-1}Ag^+-CO$ are determined to be 0.92 ± 0.05, 1.13 ± 0.04, 0.57 ± 0.08, and $0.47^{+0.19}_{-0.04}$ for $x = 1-4$, respectively. The energies for loss of one CO from the mono- and dicarbonyls of both metal ions disagree with one set of theoretical values, but those for $Ag(CO)_x^+$ ($x = 1-3$) are in excellent agreement with more recent theoretical predictions and help verify the trends in stability found for these complexes in recent synthetic studies. Trends in bond dissociation energies with increasing ligation are discussed for both systems and compared to those for isoelectronic $Ni(CO)_x$ and $Co(CO)_x^-$ complexes.

Introduction

Metal carbonyl chemistry, more than a century old, recently received renewed attention with the synthesis of the first thermally stable homoleptic noble metal carbonyl cations.[1] Although chemisorption of CO onto copper and silver films has been reported several times,[2] until these recent studies, discrete neutral binary carbonyl complexes of these metals had only been characterized by employing matrix-isolation techniques.[3,4] After some early claims for the synthesis of the $CuCO^+$ cation,[5,6] Strauss and co-workers have succeeded in the isolation and crystallographic characterization of the silver carbonyl complexes, $Ag(CO)_x^+$ ($x = 1$ and 2), by using weakly coordinating counteranions.[7] The same group has also reported infrared and manometric evidence for the formation of the $Ag(CO)_3^+$ ion at high pressures of CO.[8] Aubke and co-workers have described the first thermally stable $Au(CO)_2^+$ complex.[9] A striking feature of these cationic complexes is the fact that the CO stretching frequencies are shifted to considerably higher energies compared to free CO, indicating a lack of back bonding from the metal to the CO ligand, which acts as a pure Lewis base. These results are supported by recent high-level ab initio calculations by Barnes, Rosi, and Bauschlicher (BRB)[10] as well as Veldkamp and Frenking (VF).[11] The latter calculations predict that the dissociation energy for loss of one CO is higher for the dicarbonyls than for the monocarbonyls, but much lower for the tricarbonyls. This helps explain the experimental difficulties encountered in isolating the $Ag(CO)_3^+$ complex.

In recent studies, we have demonstrated that guided ion beam mass spectrometry is a useful tool to obtain accurate sequential bond dissociation energies (BDEs) for $M(CO)_x^+$ species (M = V,[12] Cr,[13] Fe,[14] Ni[15]). Here, we apply this technique to determine the sequential BDEs for $Cu(CO)_x^+$ and $Ag(CO)_x^+$ ($x = 1-4$) ions. As solvation effects are absent, the gas phase is an ideal environment for detailed study of these highly reactive species. Such studies aim to provide experimentally determined BDEs for comparison with theory and the recent synthetic findings mentioned above. This work is also part of an ongoing effort[12-15] in our laboratory to understand both the periodic trends in the bonding of metal carbonyls as well as the possible changes in structure and bonding that occur with variation in ligation around the metal ion.

Experimental Methods

General. Complete descriptions of the apparatus and experimental procedures are given elsewhere.[16,17] Production of ligated copper and silver ions is described below. The ions are extracted from the source, accelerated, and focused into a magnetic sector momentum analyzer for mass analysis. Mass-selected ions are slowed to a desired kinetic energy and focused into an octopole ion guide that radially traps the ions. The octopole passes through a static gas cell containing the neutral reactant, Xe, at relatively low pressures (0.05−0.20 mTorr). After exiting the gas cell, product and unreacted beam ions drift to the end of the octopole where they are directed into a quadrupole mass filter

[⊗] Abstract published in *Advance ACS Abstracts*, March 15, 1995.

(1) Weber, L. *Angew. Chem., Int. Ed. Engl.* **1994**, *33*, 1077.
(2) Eischens, R. P.; Pliskin, W. A.; Francis, S. A. *J. Chem. Phys.* **1954**, *22*, 1786. Pritchard, J.; Sims, M. L. *Trans. Faraday Soc.* **1963**, *59*, 437. Bagus, P. S.; Hermann, K.; Steel, M. *J. Vac. Sci. Technol.* **1981**, *18*, 435.
(3) Huber, H.; Kündig, E. P.; Moskovits, M.; Ozin, G. A. *J. Am. Chem. Soc.* **1975**, *97*, 2097. Kasai, P. H.; Jones, P. M. *J. Am. Chem. Soc.* **1985**, *107*, 813. Chenier, J. H. B.; Hampson, C. A.; Howard, J. A.; Mile, B. *J. Phys. Chem.* **1989**, *93*, 114.
(4) McIntosh, D.; Ozin, G. A. *J. Am. Chem. Soc.* **1976**, *98*, 3167.
(5) Scott, A. F.; Wilkening, L. F.; Rubin, B. *Inorg. Chem.* **1969**, *8*, 2533.
(6) Desjardins, C. D.; Edwards, D. E.; Passmore, *Can. J. Chem.* **1979**, *57*, 2714.
(7) Hurlburt, P. K.; Anderson, O. P.; Strauss, S. H. *J. Am. Chem. Soc.* **1991**, *113*, 6277. Hurlburt, P. K.; Rack, J. J.; Dec, S. F.; Anderson, O. P.; Strauss, S. H. *J. Am. Chem. Soc.* **1993**, *115*, 373. Hurlburt, P. K.; Rack, J. J.; Luck, J. S.; Dec, S. F.; Webb, J. D.; Anderson, O. P.; Strauss, S. H. *J. Am. Chem. Soc.* **1994**, *116*, 10003.
(8) Rack, J. J.; Moasser, B.; Gargulak, J. D.; Gladfelter, W. L.; Hochheimer, H. D.; Strauss, S. H. *J. Chem. Soc., Chem. Commun.* **1994**, 685.
(9) Adelhelm, M.; Bacher, W.; Höhn, E. G.; Jacob, E. *Chem. Ber.* **1991**, *124*, 1559. Willner, H.; Schaebs, J.; Hwang, G.; Mistry, F.; Jones, R.; Trotter, J.; Aubke, F. *J. Am. Chem. Soc.* **1992**, *114*, 8972.
(10) Barnes, L. A.; Rosi, M.; Bauschlicher, C. W., Jr. *J. Chem. Phys.* **1990**, *93*, 609.
(11) Veldkamp, A.; Frenking, G. *Organometallics* **1993**, *12*, 4613.
(12) Sievers, M.; Armentrout, P. B. *J. Phys. Chem.* accepted for publication.
(13) Khan, F. A.; Clemmer, D. E.; Schultz, R. H.; Armentrout, P. B. *J. Chem. Phys.* **1993**, *97*, 7978.
(14) Schultz, R. H.; Crellin, K. C.; Armentrout, P. B. *J. Am. Chem. Soc.* **1991**, *113*, 8590.
(15) Khan, F. A.; Steele, D. L.; Armentrout, P. B. *J. Phys. Chem.* in press.
(16) Ervin, K. M.; Armentrout, P. B. *J. Phys. Chem.* **1985**, *83*, 166.
(17) Schultz, R. H.; Armentrout, P. B. *Int. J. Mass Spectrom. Ion Processes* **1991**, *107*, 29.

0002-7863/95/1517-4071$09.00/0

for mass analysis and then detected. Ion intensities are converted to absolute cross sections as described previously.[16] Absolute uncertainties in cross sections are about 20%; relative uncertainties are 5%.

Laboratory ion energies are related to center-of-mass (CM) frame energies by $E(\mathrm{CM}) = E(\mathrm{lab})\, m/(M+m)$ where M and m are the masses of the ion and neutral reactant, respectively. The absolute energy scale and the corresponding full width at half maximum (fwhm) of the ion beam kinetic energy distribution are determined by using the octopole as a retarding energy analyzer, as described previously.[16] The absolute uncertainty in the energy scale is 0.05 eV (lab). The energy distributions are nearly Gaussian with a fwhm of 0.2−0.4 eV (lab).

Ion Source. The $Cu(CO)_x^+$ and $Ag(CO)_x^+$ species are formed in a 1 m long flow tube operated with a mixture of 90% He and 10% Ar at a total pressure of 500−800 mTorr. Metal ions are generated in a continuous dc discharge by argon ion sputtering of a cathode consisting of a copper rod or a tantalum "boat" containing silver metal. Typical operating conditions of the cathode are negative voltages of 1−3 kV. O_2 is admitted several centimeters downstream at a pressure of ~2 mTorr to remove excited state Ag^+ ions by an exothermic reaction to form the metal oxide ions.[18] CO is then introduced to the flow 50 cm downstream from the dc discharge and the desired cluster species are formed by three-body collisions. While traversing the remaining 50 cm length of the flow tube, the metal carbonyl ions undergo ~10^5 collisions with the carrier gases. Their internal energy distribution is therefore believed to be thermalized to 300 K, the temperature of the flow tube. Previous work on a number of systems[13,14,19,20] is consistent with the production of thermalized ions under similar conditions.

Data Analysis. In our recent study of the collision-induced dissociation (CID) of $Fe(CO)_x^+$ ions,[14] we examined several systematic effects on deriving accurate thermodynamic information from CID thresholds. These effects include (a) internal excitation of reactant ions above thermal, (b) multiple collisions with Xe, (c) thermal energy of the reactant ions that might contribute to the measured thresholds, and (d) the lifetime of the dissociating ions. Here, we account for each of the factors mentioned above as follows.

First, the ions that traverse the 1 m flow tube are very likely thermalized by the 10^5 collisions they undergo, such that excess internal excitation is unlikely. Second, effects due to multiple collisions with Xe are examined by performing the experiments at two different pressures of about 0.18 and 0.05 mTorr for all ions. Pressure effects are eliminated, following a procedure developed previously,[21] by linearly extrapolating the cross sections to zero-pressure, rigorously single collision conditions. It is these extrapolated cross sections that are further analyzed, except for $CuCO^+$, $AgCO^+$, and $Ag(CO)_4^+$, cases in which no pressure dependence of the cross sections was observed.

Third, we showed in our study of $Fe(CO)_x^+$ ions[14] that a very important systematic effect on CID thresholds is the rotational and vibrational energy of the thermalized ions. Because the rotational energy distribution is relatively narrow, we simply add the average rotational energy (kT = 0.026 eV for linear ions and $3kT/2$ = 0.039 eV for nonlinear ions at 298 K) to the measured threshold. The vibrational energy of the ions is best handled by explicitly considering the entire distribution of populated vibrational states. The model used to reproduce the experimental cross section is then given by eq 1,

$$\sigma(E) = \sigma_0 \sum g_i (E + E_{\mathrm{rot}} + E_i - E_0)^n / E \qquad (1)$$

where E is the relative collision energy, E_{rot} is the rotational energy of the reactants, E_0 is the reaction threshold at 0 K, and n is an adjustable parameter. The summation is over the vibrational states i having energies E_i and populations g_i, where $\sum g_i = 1$. We assume that the relative reactivity, as reflected by σ_0 and n, is the same for all vibrational states. Details of our implementation of this equation are given elsewhere.[14] Briefly, the Beyer−Swinehart algorithm[22] is used to evaluate the density of the ion vibrational states, and then the relative populations g_i are calculated by the appropriate Maxwell−Boltzmann distribution at 300 K.

Table 1. Vibrational Frequencies for $Cu(CO)_x^+$ and $Ag(CO)_x^+$ Species[a]

species		frequencies, cm^{-1} (degeneracies)
CO		2143
$CuCO^+$ [b]		2416, 270 (2), 240
$Cu(CO)_2^+$ [b]		2423, 2417, 303, 299 (2), 273 (2), 217, 52 (2)
$Cu(CO)_3^+$		2383 (3), 259 (2), 246, 217, 213 (2), 198 (2), 185, 44, 20 (2)
$Cu(CO)_4^+$ [c]	(A)	2132, 2058 (3), 459 (3), 423 (3), 380 (2), 371, 300 (3), 79 (3), 62 (2)
	(B)	2132, 2058 (3), 344 (3), 317 (3), 285 (2), 278, 225 (3), 59 (3), 47 (2)
$AgCO^+$ [d]		2177, 207 (2), 201
$Ag(CO)_2^+$ [d]		2180 (2), 281, 260 (2), 230 (2), 209, 47 (2)
$Ag(CO)_3^+$ [d]		2166 (2), 2165, 235 (2), 224, 197, 194 (2), 180 (2), 168, 40, 18 (2)
$Ag(CO)_4^+$	(A)	2132, 2058 (3), 399 (3), 368 (3), 331 (2), 323, 261 (3), 69 (3), 54 (2)
	(B)	2132, 2058 (3), 299 (3), 276 (3), 248 (2), 242, 196 (3), 51 (3), 41 (2)

[a] Degeneracies in parentheses. A and B refer to independent sets of estimated frequencies. [b] Based on theoretically calculated vibrational frequencies in ref 10. [c] Based on $Ni(CO)_4$ vibrational frequencies in ref 23. [d] Based on theoretically calculated vibrational frequencies in ref 11.

The vibrational frequencies of the $Cu(CO)_x^+$ and $Ag(CO)_x^+$ ions used in our modeling are given in Table 1. For $CuCO^+$ and $Cu(CO)_2^+$ ions, we use the vibrational frequencies calculated by BRB,[10] and for $Ag(CO)_x^+$ (x = 1−3), we choose those computed by VF.[11] Scaling of the $CuCO^+$ and $Cu(CO)_2^+$ frequencies by a factor of 1.05 (estimated by the difference in the value for free CO calculated by BRB, 2265 cm^{-1}, versus an experimental value of 2143 cm^{-1})[10] has no effect on our threshold analysis. Likewise, the use of the experimentally observed CO stretching frequencies for $Ag(CO)_2^+$ (2220 and 2196 cm^{-1}) and $Ag(CO)_3^+$ (2192 cm^{-1})[7] instead of the theoretical ones in Table 1 does not change our results. In all cases, these frequencies are much too high to be appreciably populated at 300 K and therefore the results do not depend on the exact choice of the values.

For the other species studied experimentally, $Cu(CO)_x^+$ (x = 3 and 4) and $Ag(CO)_4^+$, the vibrational frequencies must be estimated. Those for $Cu(CO)_3^+$ are estimated from the $Ag(CO)_3^+$ frequencies based on comparison of the frequencies of the mono- and dicarbonyl species of both metals. For $Cu(CO)_4^+$, we consider two different sets of frequencies as upper and lower bounds consisting of the known vibrational frequencies of $Ni(CO)_4$ (set A)[23] and these values with the metal ligand frequencies reduced by 25% (set B). Values for $Ag(CO)_4^+$ are obtained by relating its metal−ligand stretching frequencies to those of $Cu(CO)_4^+$ by a relationship based on a Morse potential, $[(\mu/D_e)_{Ag}/(\mu/D_e)_{Cu}]^{1/2} \approx 0.87$, where μ and D_e are the reduced mass and the bond energies, respectively. The D_e values were determined by fitting the data in an iterative procedure starting with the vibrational frequencies of $Ni(CO)_4$. To determine the other metal−ligand vibrational frequencies for $Ag(CO)_4^+$, corresponding values from both sets of $Cu(CO)_4^+$ frequencies were reduced by the factor 0.87. The use of the same factor for stretches, bends, and torsions is consistent with the relative frequency values for the mono- and dicarbonyls of Cu^+ and Ag^+.

Finally, we explicitly examine lifetime effects on the thresholds by considering whether all ions with energies in excess of the dissociation energy dissociate within our experimental time window. The dissociation of $Cu(CO)_x^+$ and $Ag(CO)_x^+$ species must occur during the flight time from the gas cell to the quadrupole mass filter that is used for

(18) Chen, Y.-M.; Armentrout, P. B. *J. Chem. Phys.* Submitted for publication.

(19) Fisher, E. R.; Armentrout, P. B. *J. Chem. Phys.* **1991**, *94*, 1150. Fisher, E. R.; Kickel, B. L.; Armentrout, P. B. *J. Chem. Phys.* **1992**, *97*, 4859. Dalleska, N. F.; Honma, K.; Armentrout, P. B. *J. Am. Chem. Soc.* **1993**, *115*, 12125.

(20) Dalleska, N. F.; Honma, K.; Sunderlin, L. S.; Armentrout, P. B. *J. Am. Chem. Soc.* **1994**, *116*, 3519.

(21) Hales, D. A.; Lian, L.; Armentrout, P. B. *Int. J. Mass Spectrom. Ion Processes* **1990**, *102*, 269.

(22) Beyer, T.; Swinehart, D. F. *Comm. Assoc. Comput. Machines* **1973**, *16*, 379. Stein, S. E.; Rabinovitch, B. S. *J. Chem. Phys.* **1973**, *58*, 2438; *Chem. Phys. Lett.* **1977**, *49*, 183. Gilbert, R. G.; Smith, S. C. *Theory of Unimolecular and Recombination Reactions*; Blackwell Scientific Publications Ltd.: Oxford, 1990.

(23) Chase, M. W., Jr.; Davies, C. A.; Downey, J. R., Jr.; Frurip, D. J.; McDonald, R. A.; Syverud, A. N. *J. Chem. Phys. Ref. Data* **1985**, *14*, Suppl. No. 1 (JANAF Tables).

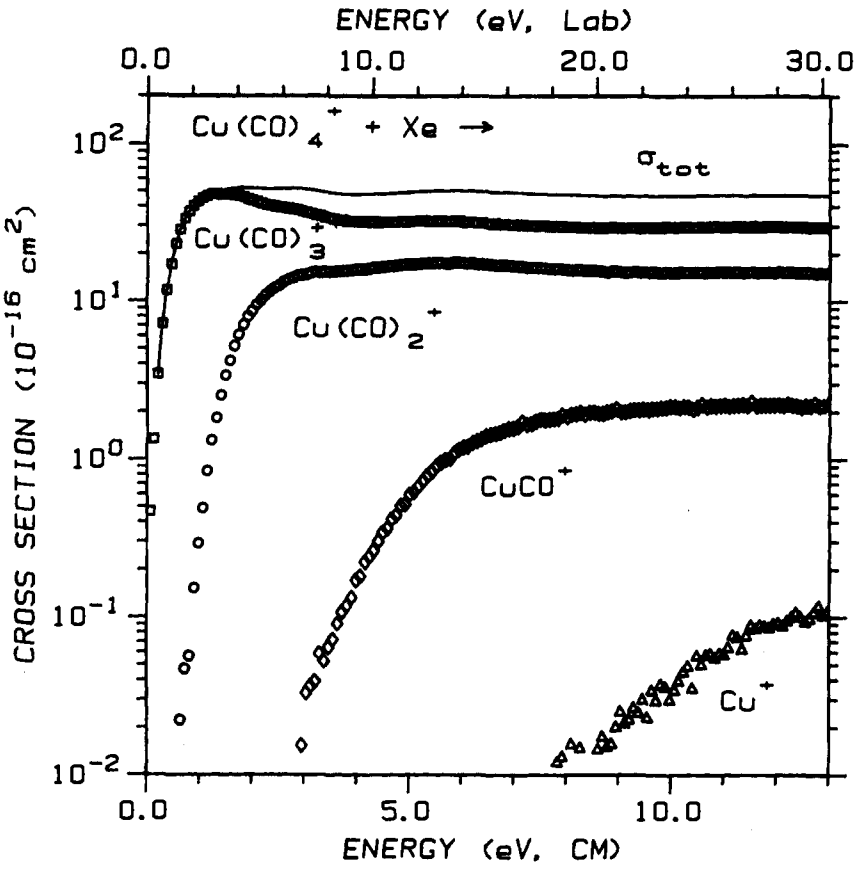

Figure 1. Cross sections for reaction of $Cu(CO)_4^+$ with Xe at 0.06 mTorr as a function of relative kinetic energy (lower x-axis) and laboratory energy (upper x-axis). Sequential loss of CO occurs to from $Cu(CO)_3^+$ (squares), $Cu(CO)_2^+$ (circles), $CuCO^+$ (diamonds), and Cu^+ (triangles). The solid line represents the total cross section for loss of CO ligands.

mass analysis. While this time does depend on the kinetic energies of the ions, it is roughly 10^{-4} s (as previously determined by time-of-flight measurements) in the threshold regions of the experiments described here. Dissociation of ions is expected to become slower as the number of vibrational modes where internal energy can randomize increases. This lifetime effect has been examined in detail in our CID experiments of $Cr(CO)_x^+$ ions.[13] Based on the analysis procedure described there and in accordance with the results for $Ni(CO)_x^+$,[15] we find that lifetime effects are fairly small, 0.01 eV for $Cu(CO)_4^+$ and $Ag(CO)_4^+$, and negligible for the tricarbonyl ions. Lifetime effects should also be negligible for smaller ions in each homologous series.

Before comparison with the experimental data, the model cross section of eq 1 (or its form that incorporates lifetime effects)[13] is convoluted over the ion and neutral translational energy distributions, as described previously.[16] The parameters in eq 1, σ_0, E_0, and n, are then optimized by using a non-linear least-squares analysis to best reproduce the data. The optimized value of E_0 is taken to be the measured threshold for a given data set. Uncertainties in the reported thresholds are derived from the spread of E_0 values from different data sets, from data obtained at different pressures (except for those species where only data extrapolated to zero pressure are analyzed, see above), from the uncertainties introduced by the choice of vibrational frequencies for the tetracarbonyl ions, and from the absolute error in the energy scale (0.05 eV in the laboratory frame).

In our analysis of $Cu(CO)_4^+$, $Ag(CO)_3^+$, and $Ag(CO)_4^+$, we also use a modified form of eq 1 that accounts for a decline in the product ion cross section at higher kinetic energies due to further dissociation. This model has been described in detail previously[24] and depends on E_D, the energy at which the dissociation channel can begin, and p, a parameter similar to n in eq 1.

Results

Analogous to previous findings in our laboratory on the collision-induced dissociation (CID) of metal carbonyl cations,[12-15] the CID of $Cu(CO)_x^+$ and $Ag(CO)_x^+$ species results in the sequential elimination of the ligand molecules. This is apparent in the data for $Cu(CO)_4^+$, shown in Figure 1, which is typical of all the copper and silver complex cations studied here. No product ions with different numbers of carbon and oxygen atoms are observed, a fact that is easily rationalized because an individual CO bond is substantially stronger than even the sum of the metal ligand bonds in $Cu(CO)_4^+$ and $Ag(CO)_4^+$. Ligand exchange reaction 2 is the only process observed other than CID.

$$CuCO^+ + Xe \rightarrow CuXe^+ + CO \qquad (2)$$

Ligand exchange also is likely to take place with $AgCO^+$ as well as $Cu(CO)_x^+$ and $Ag(CO)_x^+$ ($x \geq 2$); however, we did not measure the cross sections for the corresponding products as their masses are beyond the range of our instrument.

CID of $Cu(CO)_x^+$. Results for the interaction of $CuCO^+$ with Xe are shown in Figure 2. The Cu^+ product resulting from CID rises from an apparent threshold near 1.4 eV and reaches a maximum cross section of about 4 Å^2 at 5 eV. Ligand exchange to form $CuXe^+$ exhibits a lower apparent threshold and a cross section that peaks near the CID threshold. The latter fact is clearly due to competition between these two processes. The mass resolution of the quadrupole mass spectrometer was set sufficiently low that the cross sections shown in Figure 2 should represent the product intensities for all isotopes of Xe.

Results for the CID reaction of $Cu(CO)_2^+$ with Xe are shown in Figure 3. The cross section for the major product $CuCO^+$ has an apparent threshold similar to that for Cu^+ in Figure 2 and a magnitude about three times as large. Loss of two carbonyl ligands from $Cu(CO)_2^+$ to form Cu^+ is observed to be inefficient with a cross section rising slowly from an apparent threshold above 4.5 eV. As shown in Figure 4, the CID

(24) Weber, M. E.; Elkind, J. L.; Armentrout, P. B. *J. Chem. Phys.* **1986**, *84*, 1521.

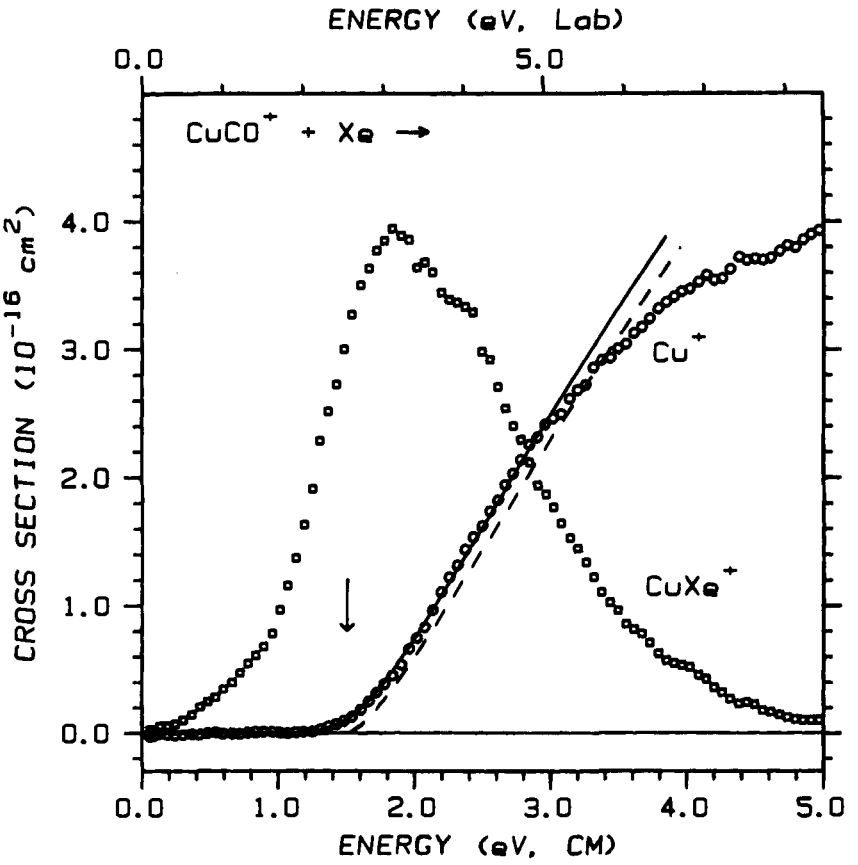

Figure 2. Cross sections for formation of Cu^+ (circles) and $CuXe^+$ (squares) from the reaction of $CuCO^+$ with Xe at a pressure of 0.06 mTorr as a function of relative kinetic energy (lower *x*-axis) and laboratory energy (upper *x*-axis). The dashed line is the model of eq 1 with the parameters in Table 2 for 0 K reactants. The solid line is this model convoluted over the translational, vibrational, and rotational energy distributions of the reactants. The arrow indicates the 0 K threshold for loss of a CO ligand at 1.54 eV.

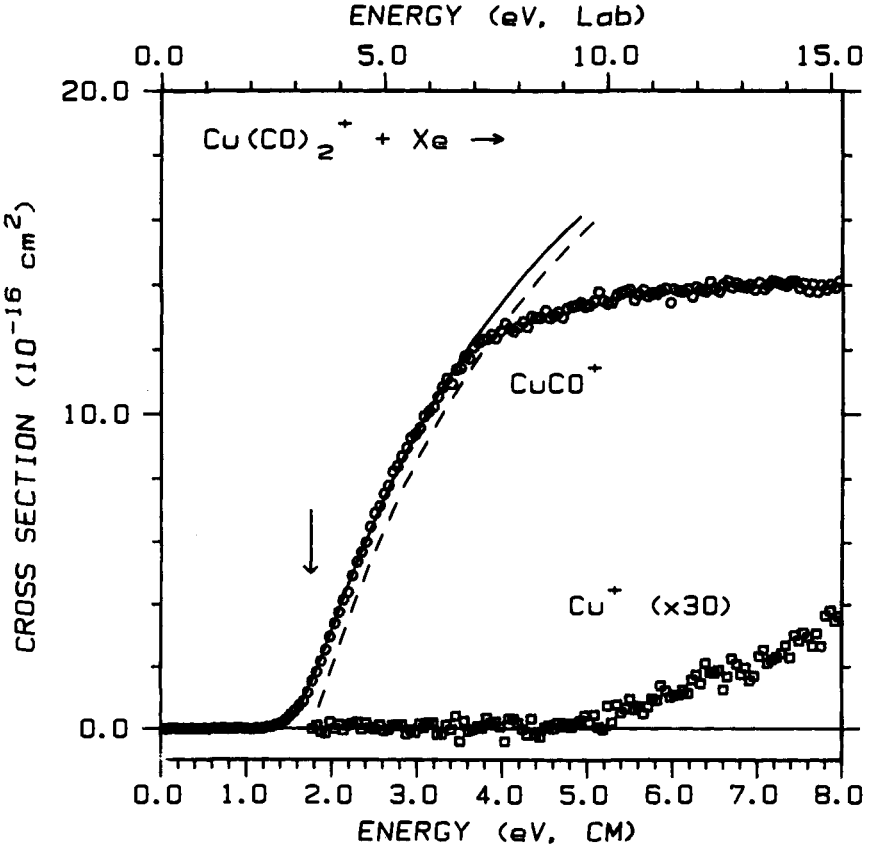

Figure 3. Cross sections for reaction of $Cu(CO)_2^+$ with Xe to form $CuCO^+$ (circles) and Cu^+ (squares, increased by a factor of 30) after extrapolation to zero pressure as a function of relative kinetic energy (lower *x*-axis) and laboratory energy (upper *x*-axis). The dashed line is the model of eq 1 with the parameters in Table 2 for 0 K reactants. The solid line is this model convoluted over the translational, vibrational, and rotational energy distributions of the reactants. The arrow indicates the 0 K threshold for loss of a CO ligand at 1.78 eV.

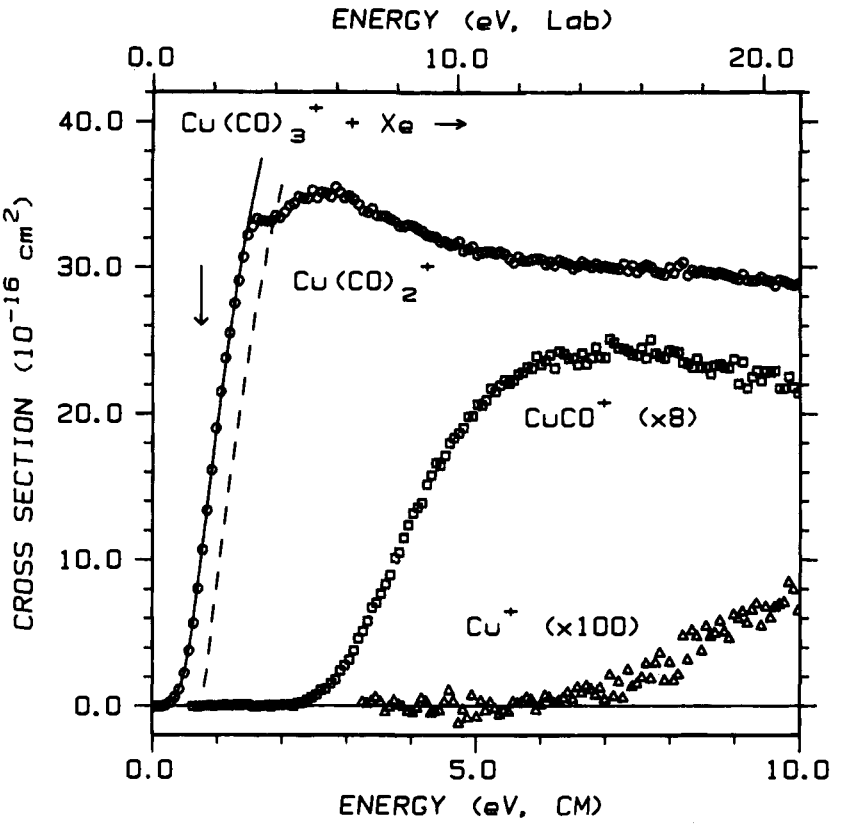

Figure 4. Cross sections for reaction of $Cu(CO)_3^+$ with Xe to form $Cu(CO)_2^+$ (circles), $CuCO^+$ (squares, increased by a factor of 8), and Cu^+ (triangles, increased by a factor of 100) after extrapolation to zero pressure as a function of relative kinetic energy (lower x-axis) and laboratory energy (upper x-axis). The dashed line is the model of eq 1 with the parameters in Table 2 for 0 K reactants. The solid line is this model convoluted over the translational, vibrational, and rotational energy distributions of the reactants. The arrow indicates the 0 K threshold for loss of a CO ligand at 0.78 eV.

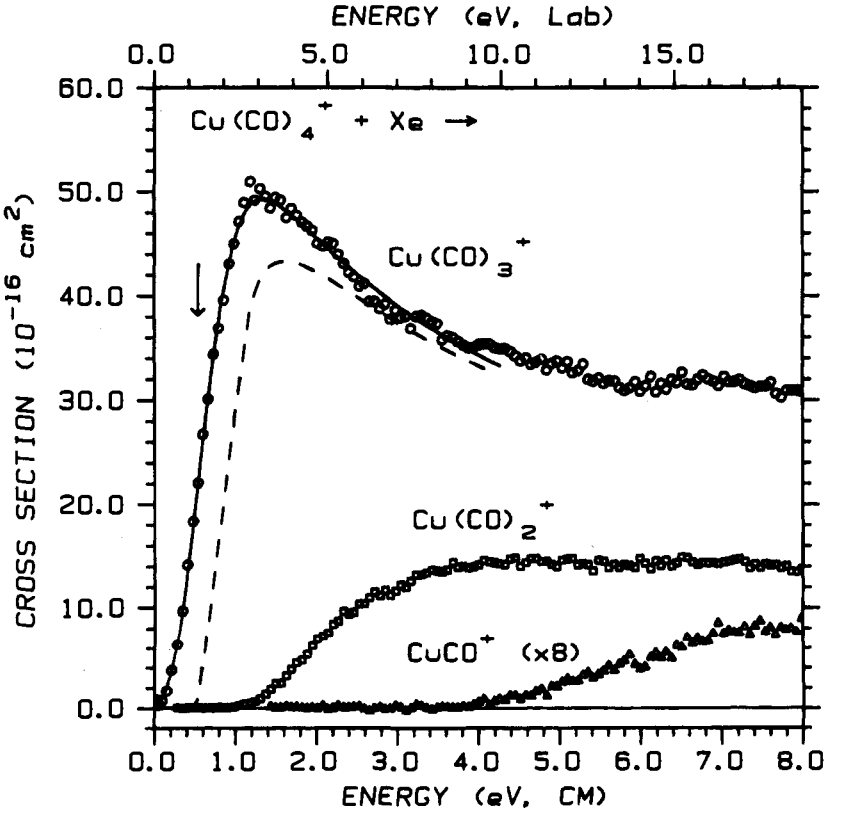

Figure 5. Cross sections for reaction of $Cu(CO)_4^+$ with Xe to form $Cu(CO)_3^+$ (circles), $Cu(CO)_2^+$ (squares), and $CuCO^+$ (triangles, increased by a factor of 8) after extrapolation to zero pressure as a function of relative kinetic energy (lower x-axis) and laboratory energy (upper x-axis). The dashed line is the model of eq 1 with the parameters in Table 2 for 0 K reactants. The solid line is this model convoluted over the translational, vibrational, and rotational energy distributions of the reactants. The arrow indicates the 0 K threshold for loss of a CO ligand at 0.55 eV.

spectrum for loss of one CO from $Cu(CO)_3^+$ exhibits a much lower apparent threshold and a substantially larger cross section than those of the two systems mentioned above. The $Cu(CO)_2^+$ product cross section goes through a maximum at the apparent threshold for the $CuCO^+$ secondary product indicating further dissociation of the former product by additional ligand loss at these higher energies. Cu^+ is again seen only at high energy and with low intensity. The CID behavior of $Cu(CO)_4^+$ is illustrated in Figures 1 and 5. The apparent threshold for loss of a single CO is even lower than in the case of the tricarbonyl complex. The $Cu(CO)_3^+$ cross section rises from near zero, peaks in a sharp maximum at the apparent onset for a second CO loss, and declines at higher energies. Consistent with the fairly constant total cross section, Figure 1, this behavior is indicative of the sequential nature of CO loss as energy is increased.

CID of $Ag(CO)_x^+$. The general appearance of these CID patterns is similar to that for the $Cu(CO)_x^+$ complexes, though the apparent thresholds for loss of one CO from the mono- and dicarbonyl compounds are considerably lower in the case of the Ag species. The interaction of $AgCO^+$ with Xe, Figure 6, shows a cross section for Ag^+ that has an apparent threshold near 0.8 eV and reaches a magnitude of ~5.5 Å^2 above 3 eV. CID of $Ag(CO)_2^+$, Figure 7, exhibits a substantially larger cross section for the loss of one CO, which also rises from an apparent threshold of about 0.8 eV. Results for the CID reactions of $Ag(CO)_3^+$ and $Ag(CO)_4^+$ with Xe are shown in Figures 8 and 9, respectively. Loss of one CO has a low apparent threshold (<0.4 eV) for $Ag(CO)_3^+$ and an even lower onset (<0.2 eV) for the tetracarbonyl complex. In contrast to $Cu(CO)_3^+$, the loss of multiple ligands from $Ag(CO)_3^+$ to form $AgCO^+$ and Ag^+ is quite efficient. Thus, the cross section for the primary product $Ag(CO)_2^+$ peaks sharply at around 1.5 eV, near the threshold for $AgCO^+$. Again, all findings are in accordance with a sequential loss of CO from these complexes as energy is increased.

BDEs from Primary Thresholds. As concluded in our previous experiments,[13-15] our best measure of the bond dissociation energies (BDEs) for $Cu(CO)_x^+$ and $Ag(CO)_x^+$ ions comes from analyses of the primary dissociation channels, reaction 3 where M = Cu or Ag.

$$M(CO)_x^+ + Xe \rightarrow M(CO)_{x-1}^+ + CO + Xe \qquad (3)$$

Optimized parameters of eq 1 obtained from analyses of reactions 3 for between two and five independent data sets for all ions are listed in Table 2. In the cases of $Ag(CO)_3^+$ and $Ag(CO)_4^+$ (Figures 8 and 9), the data for loss of a single CO can be modeled either with high of low values for n (2.5 versus 1.6 and 2.2 versus 1.1, respectively) which depend on the choice of the parameter p that describes the decline in the product ion cross sections at higher kinetic energies. These two models lead to thresholds that differ by about 0.2 eV for both systems. Both models reproduce the $Ag(CO)_4^+$ data with comparable fidelity, but the model with the higher value of n reproduces the $Ag(CO)_3^+$ cross section more accurately. On this basis and because the similar appearance of their cross sections implies that the same modeling procedure should probably be used for both systems, we believe that our best determination of the thresholds for the $Ag(CO)_3^+$ and $Ag(CO)_4^+$ systems is provided by the models with higher values of n. Further support for this choice comes from an analysis of the secondary thresholds (see below). More conservative values for these thresholds are obtained from an average of the two fits, 0.66 ± 0.12 and 0.56 ± 0.10 eV for $x = 3$ and 4, respectively.

Because the vibrational, rotational, and translational energy distributions of the reactants are explicitly included in our modeling, the thresholds of Table 2 correspond to 0 K values. Assuming that there are no activation barriers to dissociation in excess of the endothermicity, the 0 K thresholds equal $D_0[(CO)_{x-1}Cu^+-CO]$ and $D_0[(CO)_{x-1}Ag^+-CO]$. Based on theoretical considerations,[25] the long-range ion-induced dipole and ion-dipole attraction, and a kinetic energy release distribution study on the decomposition of $Mn(CO)_x^+$,[26] this is a reasonable assumption for metal carbonyl species and one that leads to accurate BDEs for other metal carbonyl systems studied previously.[13-15] In addition, there are no electronic considerations that might lead to dissociation to excited state asymptotes for the present systems, as discussed in more detail below.

Table 2. Summary of Parameters in Eq 1[a]

species	σ_0, Å^2 eV^{1-n}	E_0, eV	n
Cu^+-CO	3.3 (0.3)	1.54 (0.07)	1.5 (0.1)
$(CO)Cu^+-CO$	19 (1)	1.78 (0.03)	1.2 (0.1)
$(CO)_2Cu^+-CO$	51 (4)	0.78 (0.04)	1.4 (0.1)
$(CO)_3Cu^+-CO$	76 (5)	0.55 (0.03)	1.4 (0.1)
Ag^+-CO	6.6 (0.3)	0.92 (0.05)	1.5 (0.1)
$(CO)Ag^+-CO$	24 (1)	1.13 (0.04)	1.4 (0.1)
$(CO)_2Ag^+-CO$[b]	34 (8)	0.57 (0.08)	2.5 (0.1)
	45 (13)	0.76 (0.08)	1.6 (0.1)
$(CO)_3Ag^+-CO$[b]	15 (4)	0.47 (0.04)	2.2 (0.1)
	14 (2)	0.62 (0.04)	1.1 (0.1)

[a] Uncertainties in parentheses. [b] See text.

One possible complexity in the accurate determination of BDEs by CID methods is whether the ligand exchange reactions of $M(CO)_x^+$ with Xe (e.g. reaction 2) might cause a competitive shift in the observed thresholds, especially if cross sections for the ligand exchange processes are large or the $M(CO)_x^+$ species are complex. It should be realized that this is a general problem for all CID reactions (even though the ligand exchange product is often not collected) because the ligand exchange process will always have a lower threshold than CID, no matter what neutral reagent is used. We do not believe that this competition is likely to affect our measurements for the following reasons. First, CID reactions can occur by both indirect (transient formation of a $M(CO)_xXe^+$ complex) and direct pathways, and only the former would suffer from a competitive shift (although it can be noted that the distinction between the two pathways is primarily one of time scale, which depends on the energetics involved in the reactions). Second, competition between reaction channels can suppress the one having a higher threshold, but the true threshold can still be measured if the experiment has sufficient sensitivity. Thus, competitive shifts can be avoided if the data in the threshold region are reproduced carefully. In our studies, we attempt to accomplish this by reproducing our cross sections over a two to three order of magnitude range. In the present study, the data are reproduced over this range for $M(CO)_x^+$ ($x = 1-3$). For the $M(CO)_4^+$ species, the data are reproduced over the entire range that is available, which is only 50 because the cross sections do not actually reach zero at zero energy. Third, the cross section for the ligand exchange reaction 2 declines sharply once the CID product is formed (Figure 2). This is evidence for efficient energy transfer to the carbonyl cation upon collision with the neutral gas. Fourth, BDEs obtained from CID reactions in previous studies are generally in excellent agreement with theory and experiment for a number of metal ligand systems.[13-15,20,27] As this previous work shows similar cross sections for the ligand exchange reactions, this agreement suggests that competitive shifts are small. Conservatively, the bond energies measured

(25) Armentrout, P. B.; Simons, J. *J. Am. Chem. Soc.* **1992**, *114*, 8627.
(26) Dearden, D. V.; Hayashibara, K.; Beauchamp, J. L.; Kirchner, N. J.; van Koppen, P. A. M.; Bowers, M. T. *J. Am. Chem. Soc.* **1989**, *111*, 2401.
(27) Haynes, C. L.; Armentrout, P. B.; Perry, J. K.; Goddard, W. A., III *J. Phys. Chem.* Accepted for publication.

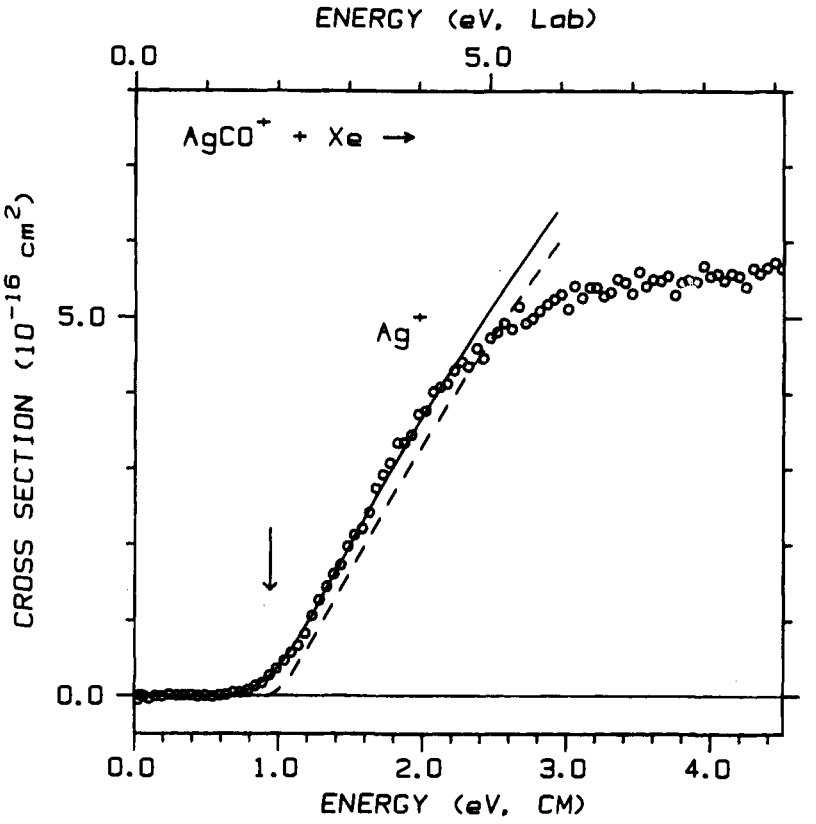

Figure 6. Cross sections for formation of Ag^+ from the reaction of $AgCO^+$ with Xe at a pressure of 0.06 mTorr as a function of relative kinetic energy (lower x-axis) and laboratory energy (upper x-axis). The dashed line is the model of eq 1 with the parameters in Table 2 for 0 K reactants. The solid line is this model convoluted over the translational, vibrational, and rotational energy distributions of the reactants. The arrow indicates the 0 K threshold for loss of a CO ligand at 0.92 eV.

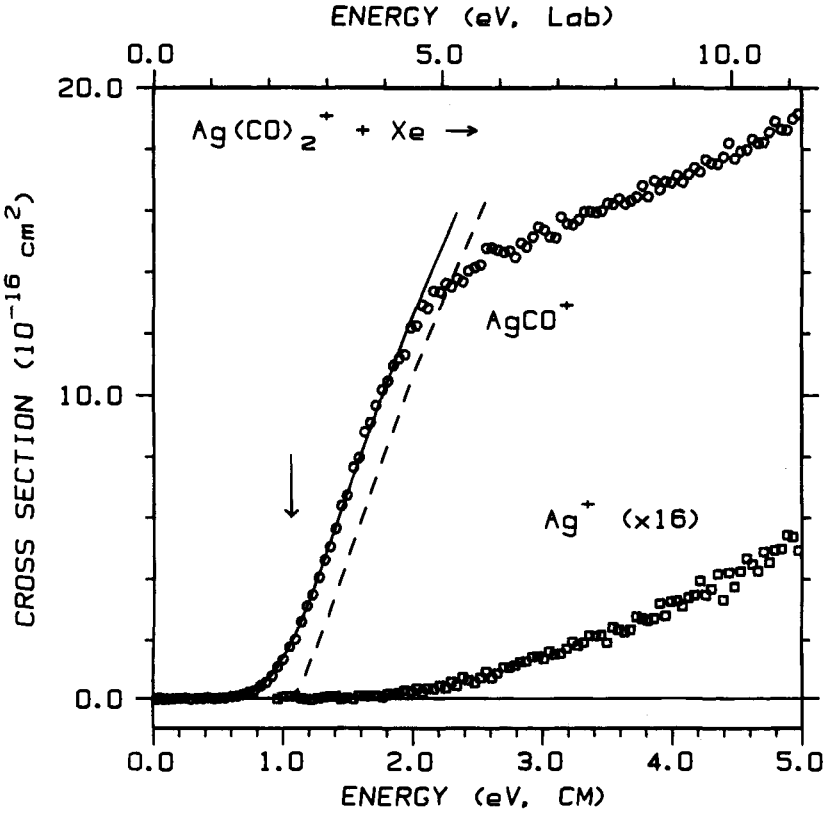

Figure 7. Cross sections for reaction of $Ag(CO)_2^+$ with Xe to form $AgCO^+$ (circles, extrapolated to zero pressure) and Ag^+ (squares, 0.06 mTorr of Xe, increased by a factor of 16) as a function of relative kinetic energy (lower x-axis) and laboratory energy (upper x-axis). The dashed line is the model of eq 1 with the parameters in Table 2 for 0 K reactants. The solid line is this model convoluted over the translational, vibrational, and rotational energy distributions of the reactants. The arrow indicates the 0 K threshold for loss of a CO ligand at 1.13 eV.

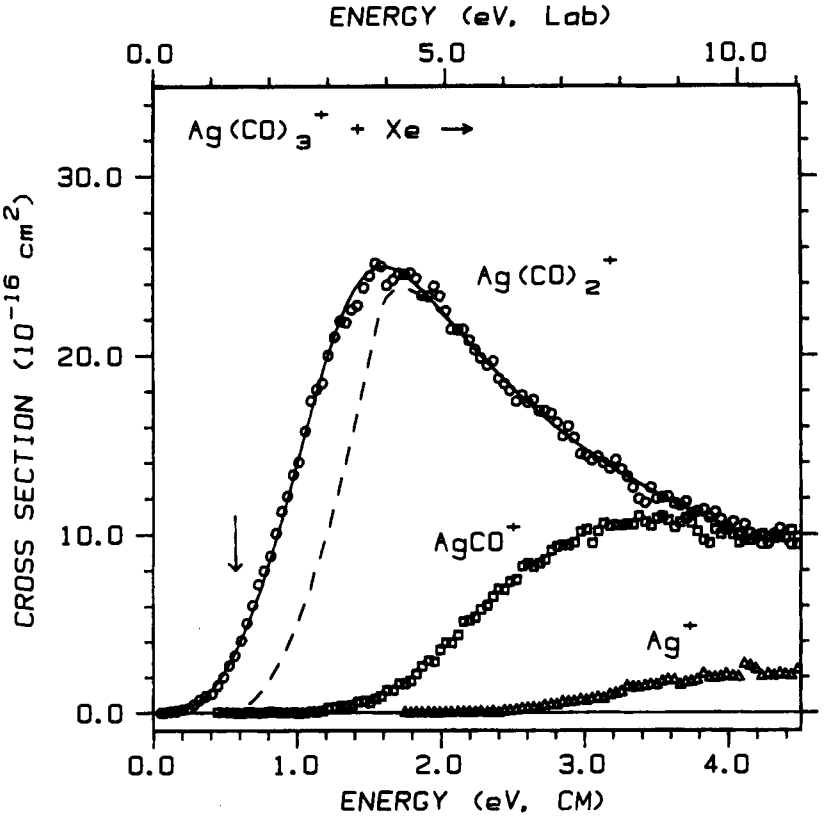

Figure 8. Cross sections for reaction of $Ag(CO)_3^+$ with Xe to form $Ag(CO)_2^+$ (circles), $AgCO^+$ (squares), and Ag^+ (triangles) after extrapolation to zero pressure as a function of relative kinetic energy (lower x-axis) and laboratory energy (upper x-axis). The dashed line is the model of eq 1 with the parameters in Table 2 ($n = 2.5$) for 0 K reactants. The solid line is this model convoluted over the translational, vibrational, and rotational energy distributions of the reactants. The arrow indicates the 0 K threshold for loss of a CO ligand at 0.57 eV.

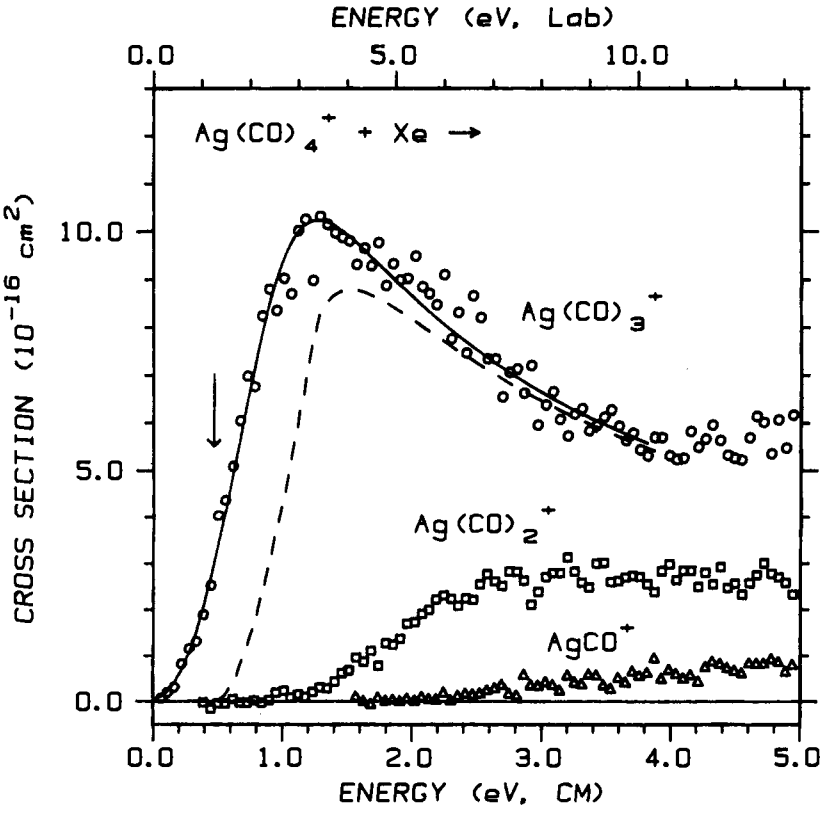

Figure 9. Cross sections for reaction of $Ag(CO)_4^+$ with Xe at a pressure of 0.17 mTorr to form $Ag(CO)_3^+$ (circles), $Ag(CO)_2^+$ (squares), and $AgCO^+$ (triangles) as a function of relative kinetic energy (lower x-axis) and laboratory energy (upper x-axis). The dashed line is the model of eq 1 with the parameters in Table 2 ($n = 2.2$) for 0 K reactants. The solid line is this model convoluted over the translational, vibrational, and rotational energy distributions of the reactants. The arrow indicates the 0 K threshold for loss of a CO ligand at 0.47 eV.

Table 3. Summary of Values for Thresholds (eV) for Loss of Two CO Ligands[a]

process	sum of primary[b]	secondary[c]
$Cu(CO)_3^+ \rightarrow CuCO^+$	2.56 (0.07)	2.44 (0.05)
$Cu(CO)_4^+ \rightarrow Cu(CO)_2^+$	1.33 (0.07)	1.42 (0.04)
$Ag(CO)_3^+ \rightarrow AgCO^+$	1.70 (0.12)[d]	1.72 (0.04)
	1.88 (0.12)[d]	
$Ag(CO)_4^+ \rightarrow Ag(CO)_2^+$	1.04 (0.12)[d]	0.9–1.6[e]
	1.37 (0.12)[d]	

[a] Uncertainties in parentheses. [b] Thresholds calculated from primary threshold energies listed in Table 2. [c] Experimental values refer to experiments performed at Xe neutral gas pressures of ~0.05 mTorr. [d] Calculated from models of the primary thresholds with a high or a low value of n, respectively. See Table 2. [e] See text.

here and in any CID study constitute upper limits to the adiabatic BDEs under investigation (assuming that energy broadening effects are adequately compensated for and the data are analyzed over an extensive energy and magnitude range); however, previous experience suggests that such CID values are likely to be accurate measures of the true bond energies.

Analyses of Secondary Thresholds. An independent means of determining the thermochemistry for these metal ion–ligand BDEs is to measure the thresholds of secondary dissociation reactions, i.e. processes 4.

$$M(CO)_x^+ + Xe \rightarrow M(CO)_{x-2}^+ + 2CO + Xe \qquad (4)$$

As discussed in greater detail in our studies on the sequential BDEs of $Cr(CO)_x^+$ and $Fe(CO)_x^+$,[13,14] thermochemical data derived from such processes generally have larger uncertainties and are less accurate than those derived from primary thresholds. This is because the secondary processes are subject to more extensive kinetic shifts (which raise the thresholds) and are more easily influenced by the multiple collision problems discussed above (which lower the thresholds). In this study, we examine these thresholds in an effort to resolve the ambiguity in the data analysis for $Ag(CO)_x^+$ (x = 3 and 4).

Data for processes 4 for the $M(CO)_x^+$ reactant species (M = Cu, x = 3 and 4; M = Ag, x = 3) at low Xe gas pressures of ~0.05 mTorr were analyzed without consideration of lifetime effects. The optimized thresholds obtained are listed in Table 3 along with the thermodynamic thresholds calculated from the primary thresholds in Table 2. The agreement between these thresholds for the two copper systems is within the combined experimental errors. The measured threshold for loss of two CO ligands from $Ag(CO)_3^+$ is in much better agreement with the thermodynamic value of 1.70 ± 0.12 eV obtained from the model with the higher value of n for the primary reaction channel of $Ag(CO)_3^+$. This lends further support for our choice of 0.57 ± 0.08 eV as our best determination of $D_0[(CO)_2Ag^+–CO]$. Unfortunately, just as for the primary dissociation channel, our experimental data for loss of two carbonyls from $Ag(CO)_4^+$ cannot be modeled in an unambiguous way. Thresholds ranging from 0.9 to 1.6 eV can be used to reproduce this cross section, consistent with either the higher or lower BDE values obtained from the primary thresholds, Table 2. Because of the ambiguity in analyzing the $Ag(CO)_4^+$ system, it seems prudent to report error limits representative of the more conservative range of reasonable fits to the data, 0.56 ± 0.10 eV. However, the similarity in the $Ag(CO)_3^+$ and $Ag(CO)_4^+$ systems strongly suggests that the lower threshold value, 0.47 ± 0.04 eV, is more likely to be accurate. Therefore, our final value is reported as $0.47^{+0.19}_{-0.04}$ eV.

Comparison with Computed BDEs. Our final values for the $M(CO)_x^+$ BDEs are listed in Table 4. No previous experimental results are available for comparison to the present results, and there are only a few ab initio studies of some of the molecular ions discussed here. After an early calculation on $CuCO^+$ by Nebot-Gil and co-workers,[28] Barnes, Rosi, and Bauschlicher (BRB) carried out a systematic study[10] on the first- and second-row transition-metal mono- and dicarbonyl cations. After correcting for zero-point energies, their results provide 0 K bond energies of 134 and 136 kJ/mol for the copper complexes and 76 and 75 kJ/mol for the silver species, respectively, Table 4. These values are considerably smaller than the ones measured in our CID experiments, by about 14 kJ/mol for the monocarbonyls and about 35 kJ/mol in the case of the dicarbonyls. We note that similar discrepancies between these theoretical and our experimental values have been found for the corresponding nickel complexes as well.[15] Furthermore, a more recent high-level computational study on the successive binding energies of $Fe(CO)_5^+$ by Ricca and Bauschlicher (RB)[29] yields significantly higher bond energies for the loss of CO from $FeCO^+$ and $Fe(CO)_2^+$ than those initially reported by BRB,[10] by 35 and 19 kJ/mol, respectively. Veldkamp and Frenking (VF)[11] obtained values of 85, 105, and 50 kJ/mol for the BDEs of $Ag(CO)_x^+$ (x = 1–3), respectively (Table 4), in excellent agreement with our experimental findings. This agreement lends additional support to our choice for the final BDE values of $Ag(CO)_x^+$ (x = 3 and 4).

Table 4. Summary of 0 K Values for $D_0[(CO)_{x-1}M–CO]$, kJ/mol[a]

species M =	x = 1	2	3	4	source
Cu^+	149 (7)	172 (3)	75 (4)	53 (3)	this work
	134	136			theory, BRB[b]
Ag^+	89 (5)	109 (4)	55 (8)[c]	45 $(^{+18}_{-4})$[c]	this work
	84.5	105.0	49.8		theory, VF[d]
	76.1	75.3			theory, BRB[b]
Ni	169 (24)	197 (24)	118 (10)	90 (2)[e]	exp, SWS[f]
	177	156	145	103	theory, PRP[g]
Co^-			159 (16)	166 (15)	exp, SWS[f]

[a] Uncertainties are reported in parentheses. [b] Reference 10. [c] More conservative values for the x = 3 and 4 BDEs are 64 ± 12 and 54 ± 10 kJ/mol, respectively. See text. [d] Reference 11. [e] Reference 36a. [f] Reference 40. These values all correspond to 298 K. [g] The values listed are taken from Table 2 of ref 36c and are those corresponding to the highest level of theory with the largest basis set for each species.

Sequential Bond Energies of $Cu(CO)_x^+$ and $Ag(CO)_x^+$. Our measured BDEs for the $Cu(CO)_x^+$ and $Ag(CO)_x^+$ (x = 1–4) complexes reveal strong nonmonotonic variations in the BDEs for loss of one CO, Figure 10. Similar nonmonotonic variations have been observed in the sequential BDEs in two related systems studied recently in this laboratory, $Fe(CO)_x^+$ (x = 1–5) and $Cr(CO)_x^+$ (x = 1–6).[13,14] There it was speculated that this might be explained in terms of changes in spin that occur when CO molecules are added to high-spin atomic metal ions to form low-spin $Fe(CO)_5^+$ and $Cr(CO)_6^+$ complexes (although the recent calculations of RB[29] belie this explanation for $Fe(CO)_x^+$ species). In contrast, sequential BDEs were found to vary *monotonically* for $Ni(CO)_x^+$ ions, which can be attributed to a lack of spin changes as CO molecules are successively added to Ni^+ to form $Ni(CO)_4^+$.[15]

Consideration of the electronic states of the copper and silver species studied here shows that spin conservation arguments cannot rationalize the observed patterns in sequential bond energies. Cu^+ and Ag^+ have $^1S(3d^{10})$ and $^1S(4d^{10})$ ground states, respectively.[30] The ground electronic states of the metal–monocarbonyl and –dicarbonyl cations have been calculated to be $^1\Sigma^+$ and $^1\Sigma_g^+$, respectively.[10,11] That of $Ag(CO)_3^+$ has

(28) Merchán, M.; Nebo-Gil, I.; Gonzáles-Luque, R.; Orti, E. *J. Chem. Phys.* **1987**, *87*, 1690.
(29) Ricca, A.; Bauschlicher, C. W., Jr. *J. Chem. Phys.* **1994**, *98*, 12899.
(30) Moore, C. E. *Natl. Stand. Ref. Data Ser., Natl. Bur. Stand.* **1971**, *35*, Vols. II and III.

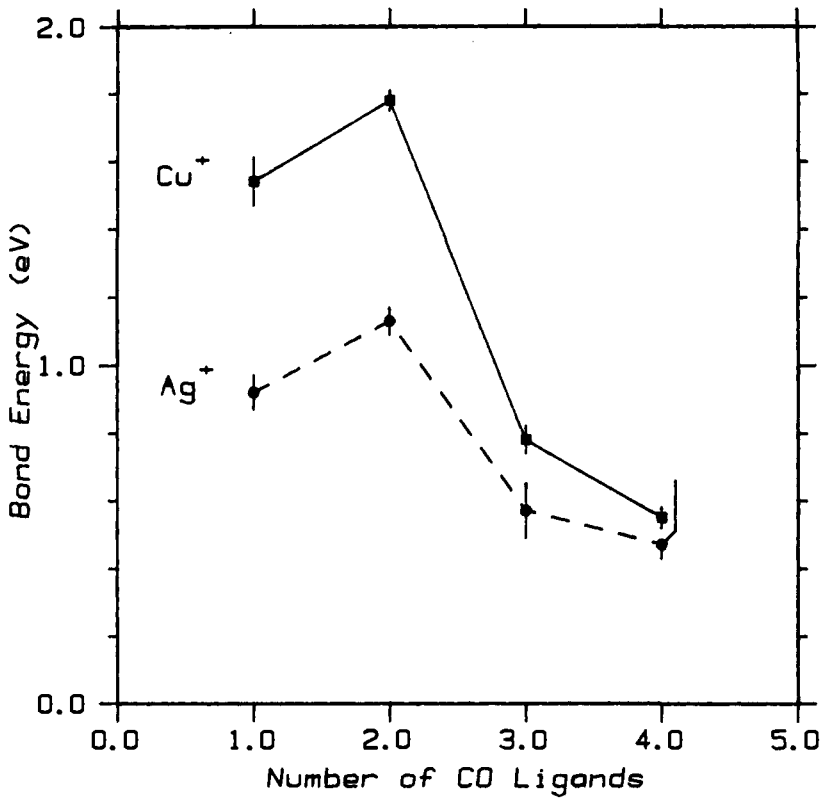

Figure 10. Bond energies for loss of CO from $Cu(CO)_x^+$ (solid squares) and $Ag(CO)_x^+$ (solid circles) as a function of the number of CO ligands. Vertical lines indicate the errors in bond energies.

been computed to be $^1A_1'$,[11] and that of $Cu(CO)_3^+$ is expected to be the same. $Cu(CO)_4^+$ and $Ag(CO)_4^+$ are undoubtedly singlet species as well. Thus, no spin changes are required as the number of CO ligands increases around the metal centers.

A trend in sequential BDEs similar to the one observed here has also been found for $Cu(H_2O)_x^+$ ($x = 1-4$).[20] Calculations on these species by Bauschlicher et al.[31] attribute the large decrease between $x = 2$ and 3 to loss of $4s-3d\sigma$ hybridization. Such hybridization removes electron density along one axis of the metal, thereby increasing the bonding to two ligands, but actually impedes addition of a third ligand. Because this hybridization requires some cost in energy, which is paid during formation of the first metal−ligand bond, the second metal−ligand bond can be stronger than the first. A similar analysis has also been used to understand a parallel sequence in the BDEs of $Co(CH_4)_x^+$ ($x = 1-3$).[27] An alternative explanation invokes π-back-bonding to the CO through the p orbitals of the metal. McIntosh and Ozin[4] used this concept to explain the nonmonotonic trends in the CO stretching frequencies observed for the neutral $M(CO)_x$ (M = Cu, Ag) complexes, that is, $f[M(CO)_3] > f[MCO] > f[M(CO)_2]$. Such π-back-bonding is unlikely to be important in the cationic systems because the promotion energy associated with going from the filled-shell d^{10} configuration to a p^1d^9 configuration for the metal cations is more than twice that for the s^1d^{10} to p^1d^{10} promotion needed in the neutral metal atoms.[30]

For the mono- and dicarbonyls, the BDEs are considerably larger (by a factor of 1.62 ± 0.07) in the Cu system than in the Ag system. These differences may be explained by two considerations. First, the ionic radius of Ag^+ is larger than that of Cu^+,[32] and hence the metal−CO bond distances are larger for the silver complexes (2.86 vs 2.50 Å measured from the metal to the center of CO).[10] From a purely electrostatic point of view, this leads to smaller BDEs for Ag^+ than for Cu^+.[33] Second, the energy difference between the $^1S(d^{10})$ ground state and the $^1D(s^1d^9)$ excited state is 3.26 eV for Cu^+ vs 5.71 eV for Ag^+.[30] Thus, the favorable $s-d\sigma$ hybridization discussed above is less easily attained in the Ag^+ system, and the enhancement in BDEs is not as large. This is also consistent with the observation that the third metal−CO BDEs (where the $s-d\sigma$ hybridization enhancement is lost) are more similar for the Cu^+ and Ag^+ systems.

The observed drop in BDEs for loss of one CO in going from $M(CO)_3^+$ to $M(CO)_4^+$ can be explained based largely on electrostatic considerations. As the number of CO ligands increases around the metal cations, so do ligand−ligand repulsions that weaken the bonds. Such effects should be less distinct for the larger Ag^+ ion, thus resulting in BDEs for $Ag(CO)_3^+$ and $Ag(CO)_4^+$ that differ by only 10 vs 22 kJ/mol for the Cu^+ systems.

Comparison with Isoelectronic Species. There are a large number of experimental and theoretical papers concerning the bond energies of neutral $Ni(CO)_x$ species,[36] isoelectronic with the $Cu(CO)_x^+$ complexes studied here. In general, the agreement among these studies is poor. The most recent theoretical numbers are listed in Table 4.[36c] Although these values differ from previous theoretical work, the differences can probably be attributed to basis set superposition errors as discussed in

(31) Bauschlicher, C. W., Jr.; Langhoff, S. R.; Partridge, H. *J. Chem. Phys.* **1991**, *94*, 2068.

(32) Wilson, R. G.; Brewer, G. R. *Ion Beams: with Applications to Ion Implantation*; Wiley: New York, 1973.

(33) The electrostatic potential of the metal ion−CO interaction is calculated as $V(r) = -e\mu\cos\theta/r^2 - \alpha e^2/2r^4$ where μ is the dipole moment of CO (0.1 D),[34] α is the parallel polarizability of CO (2.6 Å^3),[35] e is the electron charge, and θ equals 180°. With the bond distances listed in the text, this equation gives $V(Cu^+-CO) = -0.43$ eV and $V(Ag^+-CO) = -0.24$ eV. This is a ratio of 1.77, close to the experimentally observed ratio, see text.

(34) Rothe, E. W.; Bernstein, R. B. *J. Chem. Phys.* **1959**, *31*, 1619.

(35) Hirshfelder, J. O.; Curtiss, C. R.; Bird, R. B. *Molecular Theory of Gases and Liquids*; Wiley: New York, 1954; p 950.

(36) See for example: (a) Day, J. P.; Basolo, F.; Pearson, R. G. *J. Am. Chem. Soc.* **1968**, *90*, 6927. (b) Blomberg, M. R. A.; Siegbahn, P. E. M.; Lee, T. J.; Rendell, A. P.; Rice, J. E. *J. Chem. Phys.* **1991**, *95*, 5898. (c) Persson, B. J.; Roos, B. O.; Pierloot, K. *J. Chem. Phys.* **1994**, *101*, 6810.

the earlier work.[36b] Two sets of experimental values exist. The first combines appearance energy measurements for $Ni(CO)_x^-$ from Compton and Stockdale[37] with electron affinity (EA) measurements of Stevens, Feigerle, and Lineberger (SFL).[38] A more reliable set of numbers is obtained by combining the EA values of SFL with BDEs for $Ni(CO)_x^-$ ($x = 2$ and 3) measured by Sunderlin, Wang, and Squires (SWS) using CID methods.[39] This yields values for $D_{298}[(CO)Ni-CO]$ and $D_{298}[(CO)_2Ni-CO]$. $D_{298}[(CO)_3Ni-CO]$ is taken from the gas-phase ligand-exchange study of Day, Basolo, and Pearson.[36a] $D_{298}[Ni-CO]$ is then determined by subtracting these three bond energies from the sum of bond energies in $Ni(CO)_4$ as ascertained from the heats of formation for $Ni(CO)_4$, Ni, and CO. These bond energies are listed in Table 4. The key point to this progression is that the error in the value for $D[Ni-CO]$ is directly and inversely correlated with the errors in the other three bond energies, primarily that of $D[(CO)Ni-CO]$. As a consequence, while the experimental values of SWS appear to exhibit an increase in BDEs from the monocarbonyl to the dicarbonyl, a modest decrease in $D[(CO)Ni-CO]$ is directly accompanied by the same increase in $D[Ni-CO]$. Thus, the first and second experimental BDEs can easily be comparable to one another within the experimental error, in agreement with the most recent theoretical predictions.[36c] Thus, we compare the trends in our $Cu(CO)_x^+$ BDEs with the theoretical values for the sequential $Ni(CO)_x$ BDEs.

Also listed in Table 4 are the bond energies for the isoelectronic cobalt carbonyl anions, $Co(CO)_x^-$ ($x = 3$ and 4), also measured by SWS.[40] In cases where BDEs for all three metal systems are known ($x = 3$ and 4), the bond eneriges follow the ordering $D[(CO)_{x-1}Co^--CO] \geq D[(CO)_{x-1}Ni-CO] \geq D[(CO)_{x-1}Cu^+-CO]$. This trend has been noted in analogous series by SWS and can be rationalized as a difference in π-back-bonding ability of corresponding complexes with differing metal nuclear charges, and clearly shows that electrostatic effects do not dominate the bond energies.

The sequential BDEs of $D_0[M-CO]$, $D_0[(CO)M-CO]$, $D_0[(CO)_2M-CO]$, and $D_0[(CO)_3M-CO]$ for $M = Cu^+$ constitute percentages of the total binding energy of 33, 38, 17, and 12%, respectively. Those for M = Ni are 30, 27, 25, and 18%, respectively. As noted above, the trends in the $Cu(CO)_x^+$ BDEs can be rationalized largely on the basis of $s-d\sigma$ hybridization at the metal center because there are no promotion energy effects or spin changes upon ligation of Cu^+. In contrast, promotion is necessary in the Ni system because the ground state of Ni is $^3F(4s^23d^8)$, while the $Ni(CO)_x$ species are believed to have singlet ground states.[38,41] Initially, CO could bind to the lowest singlet state, $^1D(4s3d^9)$ lying 0.42 eV above the ground state, but as more ligands are added, the Ni presumably has a $3d^{10}$ configuration correlating to the $^1S(3d^{10})$ state of atomic Ni lying 1.83 eV higher than the ground state.[42] Such promotion energy effects probably explain why the first two carbonyl bonds to Ni comprise a smaller fraction of the total binding energy of $Ni(CO)_4$ than the first two ligands in the Cu^+ system. Direct comparison of the trends in the Cu^+ and Ni systems may suggest that the Ni promotion energy is paid primarily upon addition of the second carbonyl, thereby leading to a relatively weak second bond compared to that in the Cu^+ system. Alternatively, the observation that the nickel carbonyl BDEs drop monotonically could suggest that $s-d\sigma$ hybridization is not an important effect in this case. Instead, this trend could be rationalized by noting that more ligands are sharing the metal $d\pi$ electrons involved in back bonding, an effect that is not as important in the Cu^+ system, as noted above. At present, the theoretical results performed on the $Ni(CO)_4$ system do not adequately address these issues.

Conclusions

We report gas-phase measurements of sequential $Cu(CO)_x^+$ and $Ag(CO)_x^+$ ($x = 1-4$) BDEs as determined by collision-induced dissociation. Values for $M(CO)_x^+$ (M = Cu and Ag, $x = 1$ and 2) disagree with one set of theoretical values,[10] but those for $Ag(CO)_x^+$ ($x = 1-3$) are in good agreement with more recent theoretical predictions.[11] The trends in sequential BDEs are explained in terms of $s-d\sigma$ hybridization at the metal center and ligand−ligand steric interactions. Comparisons between the sequential BDEs for the isoelectronic species, $Cu(CO)_x^+$, $Ni(CO)_x$, and $Co(CO)_x^-$, provide evidence for the increasing importance of π-back-bonding as the electron density at the metal increases.

Acknowledgment. This work was supported by the National Science Foundation, Grant No. CHE-9221241. F.M. thanks the Deutsche Forschungsgemeinschaft for a fellowship. We also thank Prof. R. R. Squires for discussions concerning the $Ni-(CO)_x$ bond energies.

JA943537J

(37) Compton, R. N.; Stockdale, J. A. D. *Int. J. Mass Spectrom. Ion Phys.* **1976**, *22*, 47.
(38) Stevens, A. E.; Feigerle, C. S.; Lineberger, W. C. *J. Am. Chem. Soc.* **1982**, *104*, 5026.
(39) Sunderlin, L. S.; Wang, D.; Squires, R. R. *J. Am. Chem. Soc.* **1992**, *114*, 2788.
(40) Sunderlin, L. S.; Wang, D.; Squires, R. R. *J. Am. Chem. Soc.* **1993**, *115*, 12060.
(41) Howard, I. A.; Pratt, G. W.; Johnson, K. H.; Dresselhaus, G. *J. Chem. Phys.* **1981**, *74*, 3415.
(42) Sugar, J.; Corliss, C. *J. Phys. Chem. Ref. Data* **1985**, *14*, Suppl. No. 2.